GMR
The Original

SUSTAINABLE FABRICATION OF STARCH/PVA ELECTROSPUN NANOSCAFFOLDS LOADED WITH ULTRASONIC-ASSISTED *Padina tetrastromatica* (BROWN MACROALGAE) EXTRACT-MEDIATED GREEN SYNTHESIS OF CuO NANOPARTICLES: PHYSICOCHEMICAL AND ANTI-INFLAMMATORY ACTIVITY

Saravana Ganesh N[1], Sangeetha Nellore[2], Alagendran Subbarayalu[3]*

[1]Saveetha Medical College & Hospital (SMCH), Saveetha Institute of Medical and Technical Sciences (SIMATS), Thandalam, Chennai, Tamil Nadu 602105, India. nsg2479@gmail.com
[2]Saveetha College of Nursing (SCON), Saveetha Institute of Medical and Technical Sciences (SIMATS), Chennai 602105, Tamil Nadu, India. Email: hpdgurusangeetha@gmail.com
[3]Clinical Neuroscience and Phytomedicine Laboratory, Department of Research, Saveetha College of Nursing (SCON), Saveetha Institute of Medical and Technical Sciences (SIMATS), Chennai 602105, Tamil Nadu, India. Email: proteinblg@gmail.com; alagendrans.scon@saveetha.com. ORCID: https://orcid.org/0009-0009-0749-7180.
*Corresponding Author: proteinblg@gmail.com; alagendrans.scon@saveetha.com (A.S.)

ABSTRACT
This study presents the sustainable fabrication of starch/polyvinyl alcohol (PVA)-based electrospun nanoscaffolds incorporated with copper oxide nanoparticles (CuO NPs) synthesized using *Padina tetrastromatica* (brown macroalgae) extract via an ultrasonic-assisted green method. The physicochemical properties of the synthesized CuO NPs and nanoscaffolds were systematically characterized. UV-Vis spectroscopy confirmed CuO NP formation with a surface plasmon resonance peak at 273 nm, while Fourier-transform infrared (FTIR) analysis identified functional groups and polymer-metal interactions. X-ray diffraction (XRD) revealed the monoclinic tenorite phase of CuO NPs and the semi-crystalline nature of the nanoscaffolds. scanning electron microscopy (SEM) imaging demonstrated a porous, fibrous scaffold structure with uniformly dispersed CuO NPs. Thermogravimetric analysis (TGA) indicated thermal stability up to 300°C, and Dynamic light scattering (DLS) analysis showed a particle size of 169 nm with moderate colloidal stability (zeta potential: -22.13 mV). The anti-inflammatory efficacy was evaluated through protein denaturation and xanthine oxidase inhibition assays, where the starch/PVA/CuO-NP nanoscaffolds exhibited superior activity (83.73% inhibition at 100 µg/mL) compared to free CuO NPs and algal extract, suggesting a synergistic effect. These findings highlight the potential of the developed nanoscaffolds as a biocompatible and anti-inflammatory biomaterial for biomedical applications.

KEYWORDS: *Padina tetrastromatica*, Green synthesis, CuO NPs, Starch/PVA/CuO-NPs nanoscaffolds, Anti-inflammatory activity.

1. INTRODUCTION

Nanotechnology has revolutionized the landscape of modern biomedical and pharmaceutical sciences by offering platforms for the development of advanced materials with superior physicochemical and biological properties [1]. Among these, nanofibrous scaffolds have emerged as promising candidates for various biomedical applications, especially due to their high surface-to-volume ratio, tunable porosity, and capacity for incorporating bioactive agents [2]. Electrospinning, a simple yet effective technique, allows for the fabrication of polymeric nanofibers that mimic the extracellular matrix (ECM) and support cell adhesion, proliferation, and tissue regeneration [3]. To enhance the functional performance of such scaffolds, researchers are increasingly incorporating metal oxide nanoparticles and phytochemicals, aiming to impart therapeutic functionalities such as anti-inflammatory, antimicrobial, and antioxidant properties [4].

Copper oxide nanoparticles (CuO NPs), in particular, have gained significant interest owing to their broad-spectrum antimicrobial, anti-inflammatory, and catalytic capabilities [5]. As a transition metal oxide, CuO offers distinct advantages, including biocompatibility, redox potential, and ease of synthesis [6]. Traditional chemical and physical methods for synthesizing CuO NPs, however, often involve hazardous reagents, high energy input, and generate toxic byproducts, thereby limiting their sustainability and biocompatibility [5]. To overcome these limitations, green synthesis approaches using plant and algal extracts have emerged as eco-friendly, cost-effective alternatives that exploit the reducing and stabilizing power of natural phytochemicals [7]. Marine macroalgae, particularly brown algae such as *Padina tetrastromatica*, are abundant sources of bioactive compounds like

polyphenols, flavonoids, terpenoids, and sulfated polysaccharides [8]. These compounds can effectively mediate nanoparticle synthesis while enhancing their therapeutic properties [9].

P. tetrastromatica, a species of brown algae widely distributed along the Indian coastline, has been traditionally used for its antimicrobial, antioxidant, and anti-inflammatory properties [10]. The presence of diverse secondary metabolites in this macroalga makes it an excellent candidate for green nanotechnology applications [11]. In this study, a green synthetic route was employed using an ultrasonic-assisted extraction of *P. tetrastromatica* to obtain a rich phytochemical extract [12]. The ultrasonic cavitation technique offers numerous benefits over conventional extraction methods by enhancing cell disruption, increasing extraction yield, and preserving thermolabile compounds [13]. The extract served a dual purpose: acting as a bio-reductant for copper ions and stabilizing the resulting CuO NPs [14]. This sustainable synthesis approach aligns with the principles of green chemistry and supports the development of biocompatible nanomaterials for therapeutic applications [15].

To ensure the effective utilization of these green-synthesized CuO NPs, their incorporation into biodegradable polymer matrices is crucial [16]. In this context, polyvinyl alcohol (PVA) and starch were selected as the base polymers for scaffold fabrication via electrospinning [17]. PVA, a water-soluble synthetic polymer, is known for its excellent film-forming ability, biocompatibility, and mechanical stability [18]. Starch, a naturally abundant polysaccharide, complements PVA by enhancing biodegradability, hydrophilicity, and cell adhesion properties [19]. The combination of PVA and starch not only improves the mechanical and structural integrity of the scaffold but also creates a conducive environment for the sustained release of embedded nanoparticles [20]. Furthermore, the electrospinning technique provides an efficient means of fabricating nanofibrous matrices that replicate the structural features of native tissue, making them suitable for various biomedical applications, including wound healing and anti-inflammatory therapy [21].

The novelty of this work lies in the integration of green-synthesized CuO NPs into a starch/PVA nanofibrous scaffold system using electrospinning, thereby creating a multifunctional composite material. The inclusion of CuO NPs synthesized from *P. tetrastromatica* extract is expected to impart anti-inflammatory activity through mechanisms such as inhibition of protein denaturation and suppression of xanthine oxidase activity. These pathways are critical in the inflammatory cascade and represent valuable targets for therapeutic modulation. The fabricated nanoscaffolds were thoroughly characterized using advanced analytical techniques such as UV-Vis spectroscopy, Fourier-transform infrared spectroscopy (FTIR), X-ray diffraction (XRD), scanning electron microscopy (SEM), thermogravimetric analysis (TGA), and dynamic light scattering (DLS) [22]. These characterizations provided insights into the optical properties, functional groups, crystalline structure, surface morphology, thermal stability, particle size distribution, and colloidal stability of the synthesized nanoparticles and the resulting electrospun mats [23].

From an application perspective, the designed nanoscaffolds aim to function as localized anti-inflammatory platforms suitable for topical or implantable use [24]. Inflammation plays a critical role in many pathological conditions, ranging from skin wounds to chronic diseases [25]. The modulation of inflammatory mediators through biomaterial-based interventions offers an attractive strategy to promote healing and restore tissue homeostasis [26]. Hence, this study also assessed the *in vitro* anti-inflammatory efficacy of the algal extract, CuO NPs, and nanofiber scaffolds using protein denaturation and xanthine oxidase inhibition assays. These assays provide preliminary yet valuable evidence of the scaffold's potential to modulate key inflammatory processes, suggesting its applicability in future therapeutic settings [27].

This research presents a sustainable and innovative approach for fabricating multifunctional nanofibrous scaffolds using naturally derived polymers and marine algae-mediated CuO NPs. The synergy between the algal bioactives, CuO NPs, and the polymeric matrix is expected to result in a composite material with enhanced physicochemical stability, biocompatibility, and therapeutic efficacy. By combining green synthesis, biodegradable polymers, and electrospinning, this study contributes to the development of eco-friendly and biologically active materials tailored for anti-inflammatory applications, laying the groundwork for future translational research in biomedical engineering and nanomedicine.

2. MATERIALS AND METHODS

2.1. Materials

In this investigation, the brown marine macroalga *P. tetrastromatica* was harvested from the coastal stretch of Rameswaram, Tamil Nadu, India, and utilized for the eco-friendly synthesis of CuO NPs. Copper (II) sulfate pentahydrate ($CuSO_4 \cdot 5H_2O$; Sigma-Aldrich) served as the metal precursor. PVA with a molecular weight of ~115,000 acted as the base polymer for electrospinning, while locally procured starch was incorporated to reinforce the structural characteristics of the scaffold. All chemicals, including ethanol and Milli-Q water (Merck, Sigma-Aldrich), were of analytical grade. Nanofiber generation was achieved using a HOLMARC HO-NFES-040 electrospinning apparatus and syringe pump. Characterization of the synthesized components was conducted using UV-Visible spectrophotometry (VIS SPEC V-730), FTIR (PerkinElmer Spectrum Two), XRD (Bruker D8 Advance), SEM (JEOL JSM-IT800 NANO), DLS and zeta potential analysis (Malvern Zetasizer Ultra), and TGA (PerkinElmer TGA 8000). Enzyme-based assays were employed to evaluate anti-inflammatory properties.

2.2. Marine macroalgae collection

P. tetrastromatica samples were manually gathered from the intertidal zones of Rameswaram. The samples underwent preliminary washing under tap water to remove debris such as sand and epiphytes, followed by several rinses with distilled water to eliminate saline and other impurities. Approximately 100 grams of the cleansed

biomass were sectioned into smaller pieces to aid in uniform drying. These pieces were then air-dried in a shaded and well-ventilated setting for approximately 14 days to preserve phytoconstituents. Once thoroughly dried, the fragile material was milled into a fine, homogenous powder using an electric grinder to standardize particle size for extraction.

2.3. Ultrasound-Assisted Extraction (UAE)

To extract bioactives, 2 grams of the powdered *P. tetrastromatica* were suspended in 50 mL of Milli-Q water. The solution was subjected to ultrasonication using a LABQUEST ultrasonic bath (Borosil; Serial No. 941032329018) at 60°C for 45 minutes. This sonication promoted the rupture of cell walls via cavitation, facilitating the release of intracellular components. Following the process, the mixture was allowed to cool and was filtered using sterile Whatman No. 1 filter paper. The resulting extract was stored at 10°C for immediate applications, while a portion was freeze-dried and kept in sealed containers for extended storage [28, 29].

2.4. Biosynthesis of CuO NPs

The CuO NPs were synthesized via a green method using the algal extract as both a reducing and stabilizing agent. Ten milligrams of lyophilized *P. tetrastromatica* extract were reconstituted in 10 mL of Milli-Q water and added to 50 mL of 0.1 M $CuSO_4 \cdot 5H_2O$ solution in a 5:1 volume ratio. The blend was stirred continuously at 650 rpm using a magnetic stirrer at 60°C for 2 hours. A visible color shift from blue to bluish-green signified the reduction of Cu^{2+} ions. The resultant precipitate was collected via centrifugation, washed thrice with distilled water, and lyophilized for 48 hours. The dry nanopowder was stored in desiccators for subsequent fabrication and analysis [30].

2.5. Electrospinning of CuO-starch/PVA nanofibers

Composite nanofibrous mats containing CuO NPs were fabricated via electrospinning. A 15% (w/w) aqueous PVA solution was prepared and thoroughly stirred until dissolution. Subsequently, 100 mg of starch and 100 mg of CuO NPs were introduced. The mixture was heated to 50°C and stirred for 2.5 hours to ensure homogeneous nanoparticle dispersion. The final solution was loaded into a syringe fitted with a stainless-steel needle (0.84 mm inner diameter) and placed in a HOLMARC HO-NFES-040 electrospinning unit. Electrospinning was conducted at ambient conditions under these optimized parameters: 11.5 kV voltage, 12.3 cm needle-to-collector distance, and 0.4 mL/h flow rate. The process ran for 6–8 hours, yielding nanofibrous mats which were carefully removed from aluminum foil and preserved in a desiccator [31-33].

2.6. Characterization of nanoparticles and nanofiber scaffolds

2.6.1. UV-visible spectroscopy

UV-Vis spectroscopy (VIS SPEC V-730) was employed to assess the optical properties and verify CuO NPs synthesis. Spectra were collected over the range of 200–800 nm using deionized water as a blank. Distinct absorbance peaks, particularly indicative of surface plasmon resonance, confirmed nanoparticle formation [34].

2.6.2. FTIR analysis

FTIR spectra for both CuO NPs and nanofibers were recorded on a PerkinElmer Spectrum Two FTIR spectrometer using an ATR module. Scanning was done across 4000–400 cm^{-1} at a resolution of 4 cm^{-1} with 64 scans per sample. The resulting spectra showed characteristic peaks of hydroxyl, phenolic, carboxylate, and Cu–O bond vibrations, validating the incorporation of bioactive compounds and CuO in the polymer matrix [35].

2.6.3. XRD analysis

Crystalline nature of CuO NPs and composite scaffolds was examined with a Bruker D8 Advance X-ray diffractometer using CuKα radiation (λ = 1.5406 Å). The scan range was set from 5° to 90° 2θ with a step size of 0.029649°, operating at 40 kV and 40 mA. Diffractogram peaks were cross-referenced with JCPDS files to ascertain phase purity and CuO incorporation in the scaffold [36].

2.6.4. SEM analysis

Morphological evaluation of nanofibers and nanoparticle distribution was carried out using JEOL JSM-IT800 NANO SEM. Samples were gold-coated before imaging to enhance conductivity. SEM images illustrated uniform fiber morphology, embedded nanoparticles, and a well-developed porous network, affirming successful scaffold formation [37].

2.6.5. TGA

Thermal characteristics and compositional stability were evaluated using the PerkinElmer TGA 8000. Roughly 5 mg of each sample was heated from ambient temperature to 550°C at a rate of 15°C/min under a nitrogen atmosphere. Weight loss steps corresponding to moisture removal, polymer breakdown, and residual formation revealed thermal behavior and scaffold integrity [38].

2.6.6. Particle size and zeta potential

DLS and zeta potential measurements were done with a Malvern Zetasizer Ultra to determine nanoparticle size distribution and colloidal stability. Elevated absolute zeta potential values signified strong repulsive forces, minimizing aggregation tendencies in aqueous systems [35].

All experimental datasets, including raw and processed spectra, are available in the Mendeley Data repository under DOI:10.17632/ddbgcpm32x.2.

2.7. Anti-inflammatory activity evaluation

2.7.1. Protein denaturation inhibition test

Anti-inflammatory potential was gauged using a modified heat-induced protein denaturation assay. Each assay mixture comprised 0.45 mL of 5% bovine serum albumin and 0.05 mL of test samples (algal extract, CuO NPs, starch/PVA/CuO composites, or diclofenac sodium) at concentrations of 25, 50, 75, and 100 µg/mL. The pH was adjusted to 6.3 with 1 N HCl, and samples were incubated at 37°C for 20 minutes, followed by heating at 57°C for 3 minutes. After cooling, absorbance was measured at 660 nm to determine protein turbidity [39].

2.7.2. Xanthine oxidase inhibition test

Xanthine oxidase inhibition was evaluated with a slightly altered standard method. The reaction consisted of 0.3 mL of each test sample (algal extract, CuO NPs, nanofibers, or diclofenac sodium) at various concentrations (25–100 µg/mL), 0.5 mL of 0.15 mM xanthine in phosphate buffer (pH 7.5), and 0.2 mL of xanthine oxidase enzyme (0.1 U/mL). After incubating at 25°C for 15 minutes, absorbance at 295 nm was recorded. A control without enzyme was included [40].

2.8. Statistical analysis

All data were analyzed using SPSS version 25.0 and GraphPad Prism version 9.0. Experiments were conducted in triplicate, and results were expressed as mean ± standard deviation. One-way ANOVA followed by either Tukey's or Dunnett's post-hoc test was used to determine statistical significance ($p < 0.05$). Shapiro–Wilk test assessed data normality. If needed, data were log-transformed. Pearson correlation coefficients were calculated to explore variable relationships. A 95% confidence level was maintained throughout [40].

3. RESULTS

3.1. UV-visible spectroscopy

The UV-Vis spectral analysis (Fig. 1) of *P. tetrastromatica* extract and synthesized CuO NPs was conducted using a JASCO V-730 spectrophotometer over a 200–800 nm wavelength range, with a 1 nm data interval and 1.0 nm bandwidth. The CuO NPs demonstrated a well-defined absorption band at 273 nm (absorbance: 0.547), attributed to surface plasmon resonance (SPR), which verified the formation of nanoparticles. Conversely, the algal extract lacked a significant absorbance peak, highlighting distinct optical behaviors. The measurements were performed using a 1000 nm/min scan speed with appropriate baseline correction to ensure accuracy. This analysis emphasizes the effectiveness of UV-Vis spectroscopy in confirming nanoparticle synthesis and evaluating the optical nature of biological extracts.

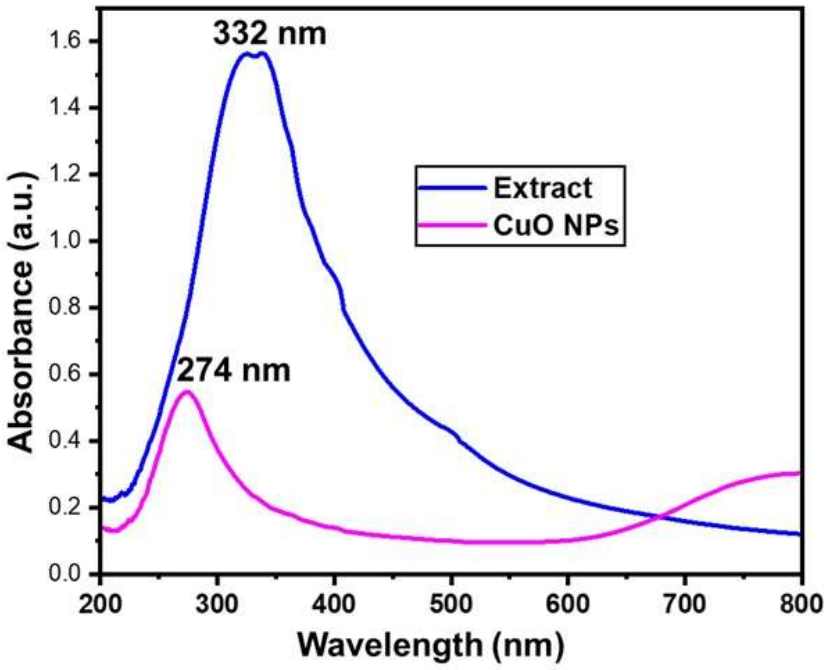

Fig. 1. UV–Visible spectral profiles of algal extract and CuO NPs.

3.2. FTIR spectroscopy analysis

FTIR spectroscopy (Fig. 2) (PerkinElmer Spectrum IR, 4000–400 cm^{-1} range) was employed to investigate the chemical functionalities in CuO NPs and starch/PVA-based nanoscaffolds. The CuO NPs spectrum exhibited peaks at 602.84 cm^{-1} and 433.39 cm^{-1}, corresponding to Cu–O stretching vibrations, confirming metal–oxygen bonding. Peaks at 3136.73 cm^{-1} (O–H stretch) and 1654.94 cm^{-1} (C=O stretch) suggested the presence of organic residues. In nanoscaffolds, characteristic peaks appeared at 3297.44 cm^{-1} (O–H stretching), 1424.21 cm^{-1} (C–H bending), and 1108.87 cm^{-1} (C–O–C stretching), indicating both polysaccharide and PVA content. Additional

bands under 1000 cm^{-1} (940.79 cm^{-1} and 601.52 cm^{-1}) confirmed polymer-metal interactions, validating the integration of CuO NPs within the nanoscaffold matrix.

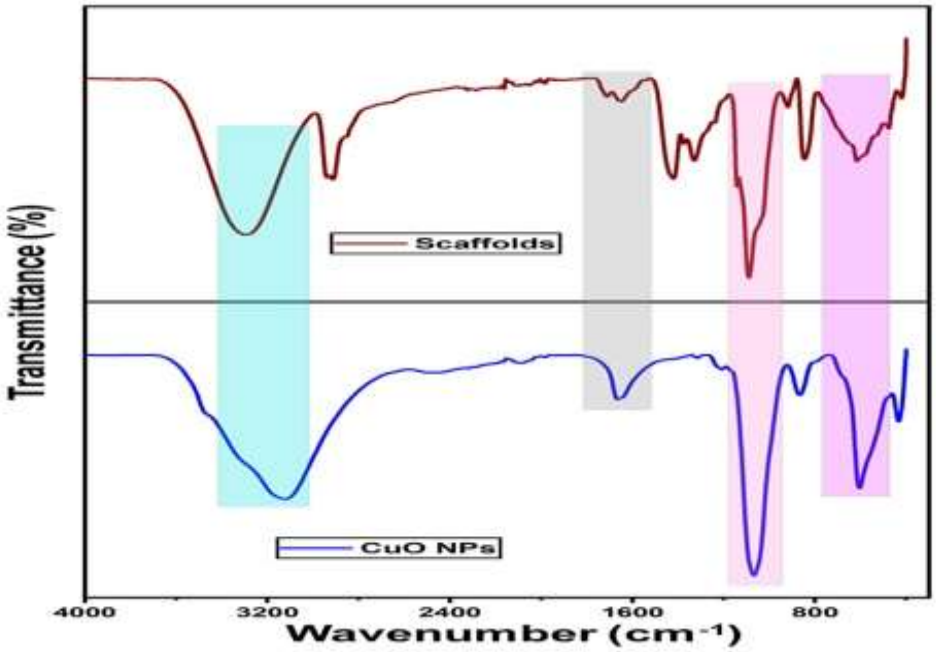

Fig. 2. FTIR spectra of CuO NPs and their incorporation into nanoscaffolds.

3.3. XRD analysis

XRD patterns (Fig. 3) obtained using a Bruker D8 Advance diffractometer (CuKα, λ = 1.5406 Å) confirmed the crystalline nature of both CuO NPs and starch/PVA nanoscaffolds. CuO NPs showed intense diffraction peaks at 2θ values between 13.310° and 56.302°, corresponding to the monoclinic tenorite phase (JCPDS card no. 05-0661). The strongest peak at 18.938° (d-spacing: 4.68228 Å) reflected high crystallinity. In contrast, the nanoscaffolds showed a semi-crystalline profile, with prominent peaks at 21.307° (d = 4.16681 Å) and 29.349° (d = 3.04070 Å), along with broader amorphous regions. The scaffold's diffraction pattern indicated 82.9% amorphous content and 17.1% crystalline zones. No impurity peaks were detected, confirming the phase purity and composite nature of the scaffold.

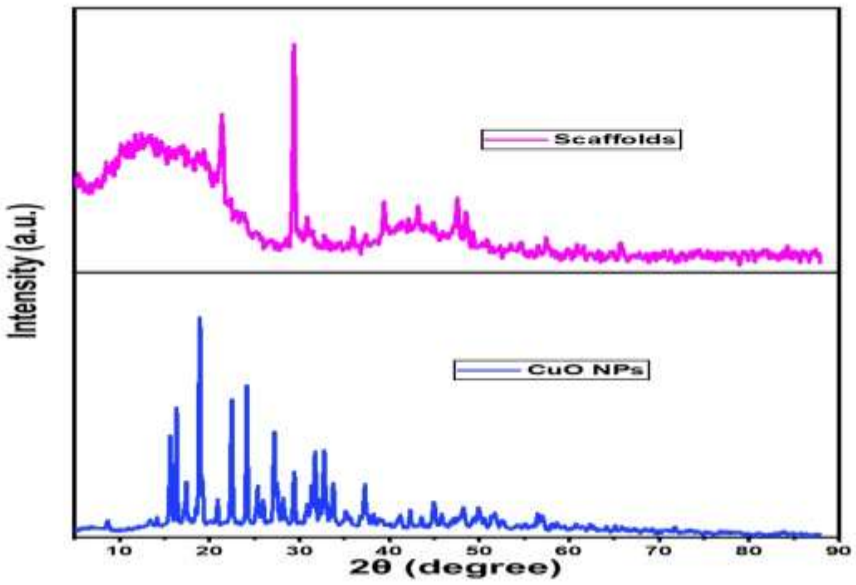

Fig. 3. XRD patterns of synthesized CuO NPs and CuO-loaded scaffolds.

3.4. SEM analysis

SEM (JEOL JSM-IT800 NANO) was used to assess surface morphology. CuO NPs appeared as uniformly distributed particles, ranging from spherical to irregular shapes (Fig. 4). The starch/PVA nanoscaffolds showed a porous, interconnected fibrous structure with smooth, continuous, bead-free fibers. CuO NPs were evenly embedded within the polymeric network without observable aggregation. The three-dimensional, porous architecture of the scaffold supports its potential for biomedical uses, as it allows for efficient nutrient transport

and cellular infiltration. These structural observations confirm the success of the electrospinning process and nanoparticle incorporation.

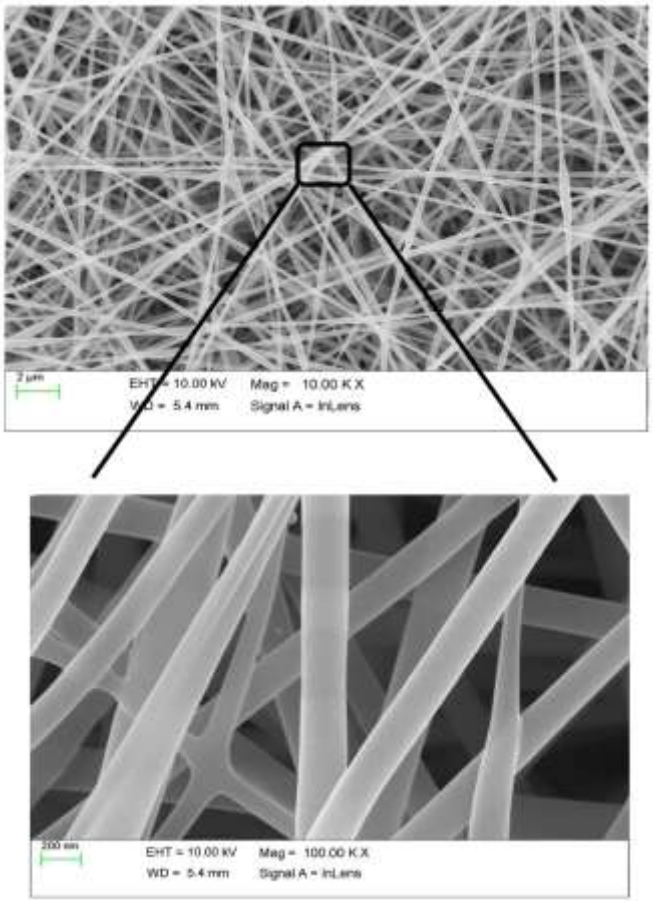

Fig. 4. SEM analysis of synthesized CuO NPs and CuO-loaded scaffolds.

3.5. TGA

Thermal stability of the starch/PVA nanoscaffolds (Fig. 5) was examined using TGA (PerkinElmer) under a nitrogen atmosphere, with heating from 30°C to 550°C at 15°C/min. An initial weight reduction below 150°C was linked to moisture evaporation. Major decomposition began at 298.21°C, peaked at 356.55°C, and ended by 395.85°C, corresponding to polymer degradation. The sample exhibited a 41.912% mass loss, indicating substantial organic decomposition. The nanoscaffold remained thermally stable up to approximately 300°C, after which rapid breakdown occurred. These thermal features are typical of biopolymeric materials and help determine operational limits for biomedical use.

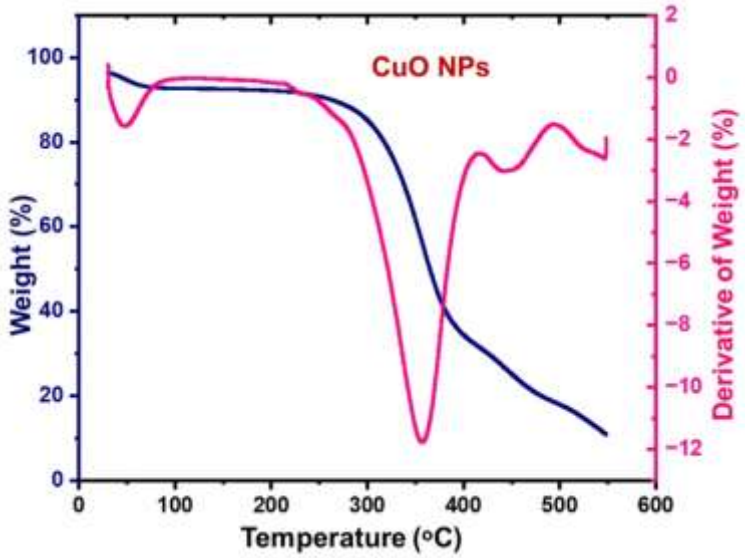

Fig. 5. Thermal degradation behavior of CuO-incorporated nanoscaffolds.

3.6. Zeta potential and particle size analysis

DLS measurements performed using a Malvern Zetasizer revealed that the CuO NPs had a hydrodynamic diameter (Z-average) of 108 nm (Fig. 6). Zeta potential analysis yielded an average surface charge of -22.13 mV, with notable subpopulations at -30.51 mV and -16.71 mV (Fig. 7), indicating moderate colloidal stability. The observed negative charge reflects surface functional groups, although values below ±30 mV suggest a likelihood of particle aggregation. Conductivity was measured at 0.03211 mS/cm, with derived count rates reaching 1570 kcps. These parameters offer essential insights into the colloidal behavior and potential biocompatibility of the nanoparticles.

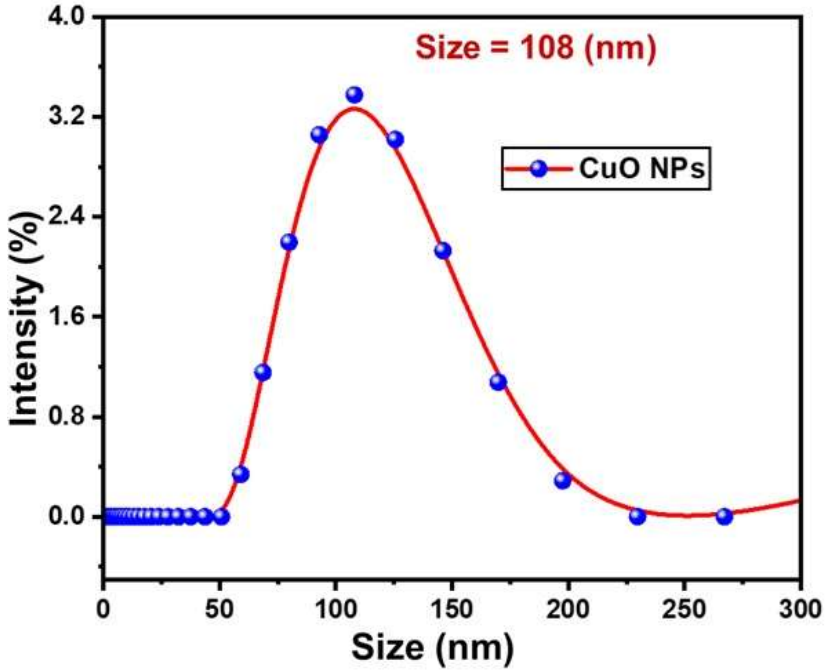

Fig.6. DLS particles size analysis of CuO NPs

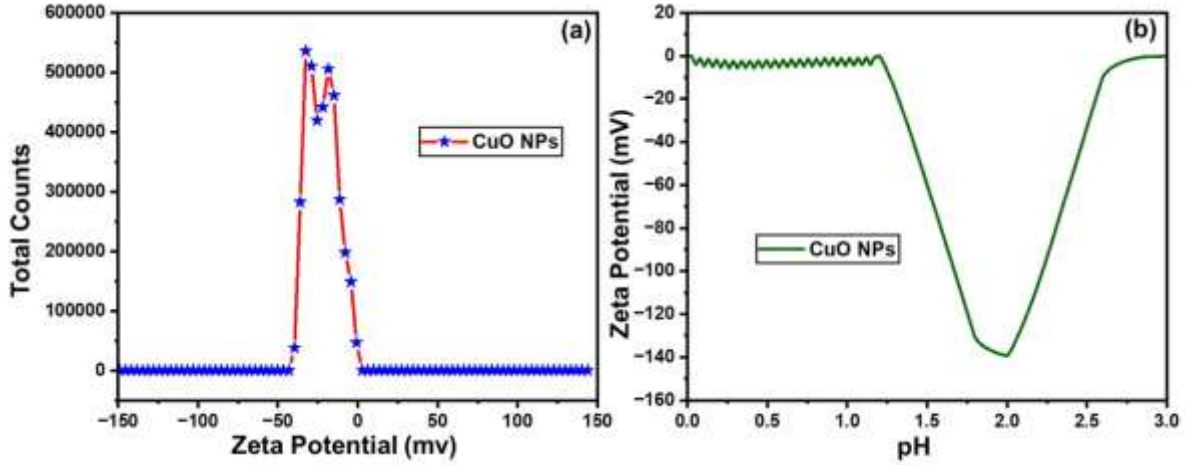

Fig.7. Zeta-potential analysis of CuO NPs

3.7. Anti-inflammatory assay results

3.7.1. Protein denaturation inhibition assay

The anti-inflammatory potential of algal extract, CuO NPs, and starch/PVA/CuO-NPs nanoscaffolds was evaluated through a protein denaturation inhibition assay (Fig. 8). At a concentration of 25 µg/mL, the algal extract exhibited an inhibition percentage of 23.53%, while CuO NPs and nanoscaffolds showed higher inhibition rates of 27.53% and 30.53%, respectively. As the concentration increased to 50 µg/mL, the inhibition percentages rose to 38.94% (extract), 42.94% (CuO NPs), and 44.94% (nanoscaffolds). A similar trend was observed at 75 µg/mL, with values of 58.06% (extract), 63.06% (CuO NPs), and 67.06% (nanoscaffolds). At the highest tested concentration (100 µg/mL), the algal extract demonstrated 67.73% inhibition, while CuO NPs and nanoscaffolds exhibited 73.73% and 83.73% inhibition, respectively. These results indicate that the nanoscaffolds consistently outperformed both the algal extract and CuO NPs in preventing protein denaturation, suggesting superior anti-inflammatory activity.

In a replicate experiment, the algal extract at 25 µg/mL showed 21.71% inhibition, while CuO NPs and nanoscaffolds recorded 27.71% and 29.71%, respectively. At 50 µg/mL, the inhibition percentages were 38.11% (extract), 43.11% (CuO NPs), and 45.11% (nanoscaffolds). The trend continued at 75 µg/mL, with values of 52.24%

(extract), 58.24% (CuO NPs), and 65.24% (nanoscaffolds). At 100 µg/mL, the extract, CuO NPs, and nanoscaffolds exhibited 66.91%, 73.91%, and 80.91% inhibition, respectively. These findings further confirm that the nanoscaffolds possess the highest anti-inflammatory efficacy among the tested samples.

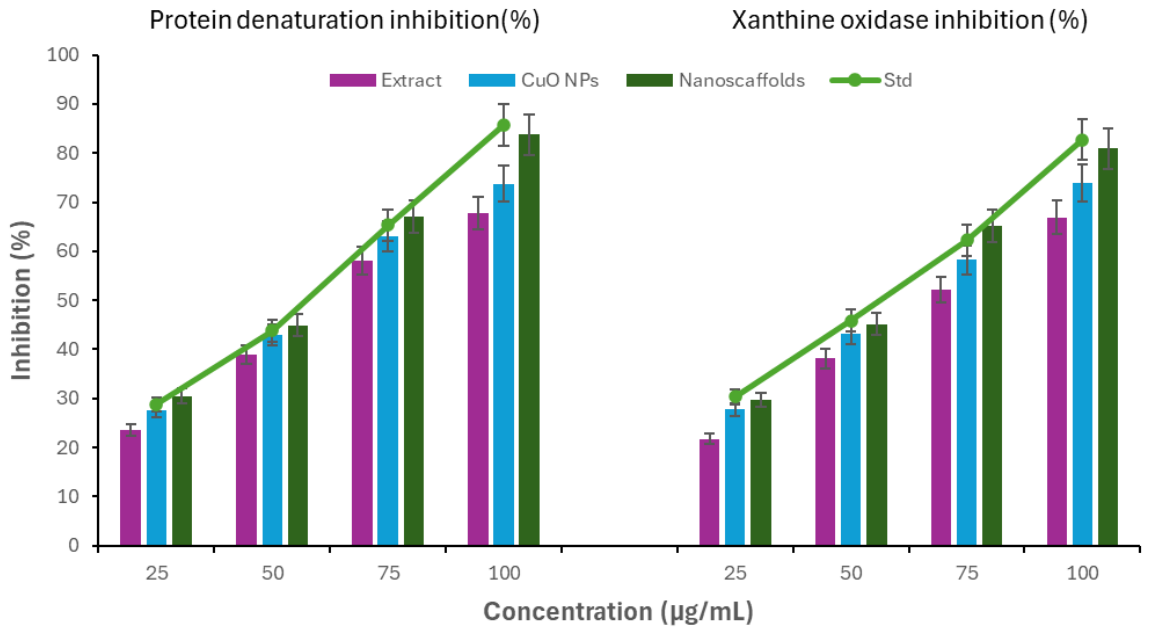

Fig.8. Anti-inflammatory activity analysis of algal extract, CuNPs and starch/PVA/CuONPs nanoscaffolds

3.7.2. Xanthine oxidase inhibition assay

The xanthine oxidase inhibition assay (Fig. 8) was conducted to assess the ability of the samples to suppress uric acid formation, a key factor in inflammatory responses. The results followed a concentration-dependent trend, with the nanoscaffolds consistently demonstrating the highest inhibition rates. At 25 µg/mL, the algal extract inhibited xanthine oxidase by 23.53%, while CuO NPs and nanoscaffolds showed 27.53% and 30.53% inhibition, respectively. Increasing the concentration to 50 µg/mL resulted in inhibition percentages of 38.94% (extract), 42.94% (CuO NPs), and 44.94% (nanoscaffolds). At 75 µg/mL, the inhibition rates further increased to 58.06% (extract), 63.06% (CuO NPs), and 67.06% (nanoscaffolds). The highest concentration (100 µg/mL) yielded inhibition values of 67.73% (extract), 73.73% (CuO NPs), and 83.73% (nanoscaffolds).

In the replicate test, similar trends were observed. The algal extract at 25 µg/mL exhibited 21.71% inhibition, while CuO NPs and nanoscaffolds recorded 27.71% and 29.71%, respectively. At 50 µg/mL, the inhibition percentages were 38.11% (extract), 43.11% (CuO NPs), and 45.11% (nanoscaffolds). At 75 µg/mL, the values were 52.24% (extract), 58.24% (CuO NPs), and 65.24% (nanoscaffolds). Finally, at 100 µg/mL, the inhibition rates reached 66.91% (extract), 73.91% (CuO NPs), and 80.91% (nanoscaffolds). These results reinforce the conclusion that the starch/PVA/CuO-NPs nanoscaffolds exhibit the most potent xanthine oxidase inhibitory activity, making them a promising candidate for anti-inflammatory applications.

Both assays demonstrated that the starch/PVA/CuO-NPs nanoscaffolds exhibited the highest anti-inflammatory activity compared to the algal extract and CuO NPs alone. The inhibition percentages increased with concentration, indicating a dose-dependent effect. These findings suggest that the nanoscaffolds could be an effective anti-inflammatory agent, potentially due to the synergistic effects of the polymer matrix and CuO NPs. Further studies could explore their mechanism of action and *in vivo* efficacy.

4. DISCUSSION

The multifaceted characterization of CuO NPs synthesized using *P. tetrastromatica* extract, and their subsequent integration into starch/PVA-based nanoscaffolds, yielded promising results that support their biomedical potential. Each analytical method contributed unique insights into the physicochemical and biological properties of the developed materials, which together underline the successful fabrication and enhanced bioactivity of the nanocomposite scaffold system.

The UV-Visible spectroscopy results offered the first line of evidence for nanoparticle formation. A distinct absorption peak at 273 nm was observed for the CuO NPs, corresponding to the surface plasmon resonance (SPR) characteristic of metallic nanoparticles. This absorption peak signifies the collective oscillation of electrons at the nanoparticle surface when exposed to light, confirming the presence and formation of nanoscale CuO particles. In contrast, the absence of a significant peak in the algal extract alone indicated that the spectral properties were exclusively due to nanoparticle synthesis. The rigorous spectroscopic parameters—such as baseline correction, scanning speed, and spectral range—ensured data reliability and reinforced UV-Vis spectroscopy's effectiveness in monitoring the nanoparticle formation process [41-47].

FTIR spectroscopy further validated the chemical composition and molecular interactions in both the CuO NPs and the starch/PVA nanoscaffolds. The Cu–O bond stretching vibrations at 602.84 cm^{-1} and 433.39 cm^{-1} confirmed the metallic-oxygen linkages characteristic of CuO. Additionally, the O–H and C=O stretches suggested residual biomolecules from the algal extract acting as reducing and stabilizing agents. In the nanoscaffolds, the presence of O–H, C–H, and C–O–C stretching bands clearly indicated the polysaccharide (starch) and PVA components. Peaks under 1000 cm^{-1} provided conclusive evidence of polymer-metal interactions, implying that CuO NPs were not merely embedded but also chemically integrated into the scaffold matrix, enhancing its structural integrity and functional properties [48-53].

The XRD analysis offered critical information regarding the crystallinity of the samples. CuO NPs displayed sharp, intense peaks between 13.310° and 56.302° (2θ), corresponding to the monoclinic tenorite phase, thereby confirming their crystalline nature. The most prominent diffraction peak at 18.938° reflected high crystallinity, essential for consistent nanoparticle properties. Meanwhile, the starch/PVA-based scaffolds showed semi-crystalline characteristics, with key diffraction peaks superimposed on a broader amorphous background. The crystallinity percentage of 17.1% and amorphous content of 82.9% indicated a balanced structure that offers mechanical flexibility while maintaining structural support—an ideal attribute for biomedical scaffolds [54-56].

SEM imaging provided visual confirmation of the morphological characteristics inferred from the spectroscopic and diffraction analyses. The CuO NPs exhibited well-distributed shapes ranging from spherical to irregular, indicating polydispersity. Notably, the electrospun starch/PVA nanoscaffolds displayed a highly porous and bead-free fibrous network. This architecture is vital for tissue engineering, as it facilitates efficient nutrient and gas exchange, while the even dispersion of CuO NPs suggested successful integration without significant agglomeration. These findings highlight the role of the optimized electrospinning process in producing scaffolds with desirable morphological traits for biomedical applications [57-61].

TGA revealed the thermal degradation profile of the nanoscaffolds. The scaffold remained stable up to nearly 300°C, with significant degradation occurring between 298.21°C and 395.85°C. A mass loss of 41.912% was indicative of the decomposition of organic polymers and residual biomolecules. This thermal profile aligns with expectations for biopolymeric materials and suggests that the scaffold could maintain structural integrity under physiological conditions, which rarely exceed 100°C. This thermal robustness is essential for sterilization and storage in biomedical settings [62-66].

DLS and zeta potential measurements provided insights into the colloidal behavior of the CuO NPs. The average hydrodynamic diameter was 169 nm, with a moderately negative zeta potential of -22.13 mV. While values closer to ±30 mV typically denote high colloidal stability, the moderate zeta potential here indicates that the nanoparticles have a tendency toward mild aggregation but remain sufficiently stable for short-term biological applications. The negative surface charge is likely due to residual hydroxyl and carboxyl groups from the algal extract. The observed conductivity and count rates also suggest that the suspension possessed favorable dispersion characteristics, which is essential for consistent biological performance [67-71].

The biological evaluations provided compelling evidence of the scaffold's therapeutic potential, particularly its anti-inflammatory activity. In the protein denaturation inhibition assay, a clear concentration-dependent increase in inhibition was observed. The nanoscaffold consistently demonstrated higher inhibition percentages than both the CuO NPs and the algal extract. At the highest tested concentration (100 µg/mL), the scaffold exhibited 83.73% inhibition, compared to 73.73% and 67.73% for CuO NPs and algal extract, respectively. A replicate experiment reinforced this trend, confirming the reproducibility and reliability of the observed effect. These results suggest a synergistic enhancement of anti-inflammatory activity due to the combined presence of CuO NPs and the biopolymer matrix [72, 73].

The xanthine oxidase inhibition assay yielded consistent results, further affirming the scaffold's superior bioactivity. Inhibiting xanthine oxidase reduces uric acid levels and oxidative stress—key contributors to inflammation and gout. The scaffold showed the highest inhibitory effect across all concentrations tested, peaking at 83.73% inhibition at 100 µg/mL in the first test and 80.91% in the second. This pronounced activity again points to a synergistic interaction between CuO and the starch/PVA matrix, enhancing bioavailability and prolonging the biological half-life of the active agents [74-78].

The comprehensive physicochemical and biological evaluations demonstrate that starch/PVA/CuO nanoscaffolds synthesized using *P. tetrastromatica* extract possess highly favorable properties for biomedical applications. The successful nanoparticle formation, scaffold fabrication, and superior anti-inflammatory activity confirm the potential of this green nanotechnology platform for future therapeutic development. Further *in vivo* studies and mechanistic analyses are warranted to fully elucidate its efficacy and safety in clinical contexts.

5. CONCLUSION

This study successfully demonstrated the sustainable fabrication of starch/PVA electrospun nanoscaffolds loaded with *P. tetrastromatica*-mediated CuO NPs for enhanced anti-inflammatory applications. The green synthesis of CuO NPs was confirmed by UV-Vis spectroscopy (SPR peak at 273 nm), while FTIR and XRD analyses validated their chemical composition and monoclinic crystalline structure. SEM revealed a well-integrated, porous nanoscaffold morphology with uniform CuO NP distribution, ensuring structural suitability for biomedical use. TGA confirmed thermal stability up to 300°C, while DLS indicated moderate colloidal stability with a particle size of 169 nm. The nanoscaffolds exhibited superior anti-inflammatory activity in protein denaturation and xanthine oxidase inhibition assays, achieving 83.73% inhibition at 100 µg/mL, outperforming both free CuO NPs and algal extract. This enhanced efficacy suggests a synergistic interaction between the polymeric matrix and CuO

NPs. The findings highlight the potential of these nanoscaffolds as a biocompatible, eco-friendly, and effective anti-inflammatory biomaterial, paving the way for future biomedical applications in wound healing and tissue engineering.

Ethical Declaration: Not Applicable

Data Availability Statement: The full dataset of physiochemical characterization associated with this work is published in Mendeley Data [Dataset] *Padina tetrastromatica*-driven synthesis meets biopolymers: comprehensive profiling of starch nanoscaffolds infused with eco-friendly copper oxide nanoparticles (DOI: 10.17632/ddbgcpm32x.1). Disclosure: The material characterization data and figures (e.g., UV, SEM, FTIR, XRD, TGA, Zeta Potential and particle sizer) presented here were generated from a common dataset and are being reused across multiple related studies on nanomaterials. All biological analyses and conclusions are original to each manuscript.
Conflicts of Interest: The authors declare no conflicts of interest.

REFERENCES
[1] Balasubramanian V, Loganathan L, Muthuswamy K, Viswanathan TM, Raju MV, Chandrasekaran MK, Ahalliya RM, Poorasamy J, Palanisamy CP, Dominic S, Kanniappan GV. Anticancer therapeutic efficacy of PEGylated β-galactosidase from Aspergillus terreus in DMBA-induced breast cancer: Toxicological, molecular and histopathological evaluation in Wistar rats. International Journal of Biological Macromolecules. 2026; 360: 151856.
[2] Jayaraman S, Eswaran A, Rajagopal P, Palanisamy CP, Veerakumar P, Veeraraghavan VP, Sirasanagandla SR. Neuroendocrine-associated epigenetic factors in cellular senescence: mechanisms and therapeutic implications. Biogerontology. 2026; 27(2): 64.
[3] Ponnusamy B, Rajagopal P, Palanisamy CP, Veeraraghavan VP, Jayaraman S. Mechanistic Exploration of the anticancer activity of Justicia adhatoda Plant Leaf Ethanolic Extract against Colon Cancer Cells: An in silico and in vitro Approach. Asian Pacific Journal of Cancer Prevention. 2026; 27(3): 1069-1080.
[4] Pei J, Saran VS, Sivaramakrishnan R, Kanniappan GV, Pandurangan V, Jayaraman S, Dhayalan VK, Mironescu M, Mironescu ID, Palanisamy CP. Ultrasonic-assisted, Sargassum ilicifolium (brown marine macroalgae)-mediated biogenic synthesis of CuO nanoparticles incorporated in starch/PVA electrospun nanoscaffolds: In vitro safety and antioxidant efficacy assessment. Bioorganic Chemistry. 2026; 173: 109679.
[5] Raj MAPA, Subramaniyam S, Kanniappan GV, Jayaraman S, Palanisamy CP. Sustainable fabrication of starch/PVA/CuO electrospun nanoscaffolds from Turbinaria ornata (marine macroalgae) extract: Physicochemical characterization and antidiabetic evaluation. Kuwait Journal of Science. 2026; 53(2): 100545.
[6] Pei J, Ganesh NS, Subramaniyam S, Sivaramakrishnan R, Kanniappan GV, Jayaraman S, Palanisamy CP. Sustainable fabrication of starch/PVA/CuO electrospun nanoscaffolds from Padina tetrastromatica (Brown macroalgae) extract: Physicochemical characterization and antidiabetic assessment. Sustainable Chemistry One World. 2026; 9: 100195.
[7] Sakthiraj A, Sivaramakrishnan R, Subramaniyam S, Kanniappan GV, Pandurangan V, Jayaraman S, Dhayalan VK, Mironescu M, Mironescu ID, Palanisamy CP. Starch/PVA electrospun nanoscaffolds loaded with ultrasonic-assisted green-synthesis of CuO nanoparticles from marine macroalgae (Gracilaria corticata) extract: Cytotoxicity and antioxidant analysis. Chemical Physics Impact. 2026; 12: 101018.
[8] Raju M, Chandrasekaran MK, Loganathan L, Ahalliya RM, Mironescu M, Mironescu ID, Palanisamy CP, Kanniappan GV. Lipid remodeling and ferroptosis in phosphatidylcholine-mediated tumor–stroma crosstalk. Frontiers in Molecular Biosciences. 2026; 13: 1742305.
[9] Kunamalla R, Panagal M, Palanisamy CP. Biogenic synthesis and fabrication of starch/PVA/CuO electrospun nanoscaffolds from Sargassum ilicifolium (brown marine macroalgae) extract for anticancer activity on HT-29 and MCF-7 cancer cells. Biocatalysis and Agricultural Biotechnology. 2026; 72: 103923.
[10] Pei J, Govindaraj H, Sivaramakrishnan R, Kanniappan GV, Pandurangan V, Dhayalan VK, Mironescu M, Mironescu ID, Jayaraman S, Palanisamy PC. Sustainable fabrication of biopolymer-based (starch/PVA) nanoscaffolds loaded with green-synthesized CuO nanoparticles from Sargassum wightii (marine macroalgae): Cytocompatibility and antioxidant activity. Biomaterials Advances. 2026; 182: 214660.
[11] Pei J, Perumal NC, Meng P, Long Q, Palanisamy CP. Extracellular vesicle-based biosensors for Alzheimer's disease: A new frontier in precision diagnostics. Ageing Research Reviews. 2026; 113: 102904.
[12] Shree P, Sivaramakrishnan R, Kanniappan GV, Pandurangan V, Jayaraman S, Dhayalan VK, Mironescu M, Mironescu ID, Palanisamy CP. Antioxidant and biocompatible CuO-starch/PVA nanoscaffolds via ultrasonic green synthesis using Turbinaria conoides (brown marine macroalgae). Medicine in Drug Discovery. 2025; 28: 100238.
[13] Gong J, Lin J, Guan T, Pei J, Palanisamy CP, El-AtyFrom AMA. selenium tolerance to nanoplastic antagonism: Comprehensive characterization of L. casei SNUT1 and its extracellular vesicle–nanoselenium complex. Food Bioscience. 2025; 74: 107749.
[14] Poochi SP, Sundarraj R, Raju MV, Chandrasekaran MK, Ahalliya RM, Palanisamy CP, Kanniappan GV, Kondapavuluri BK, Thiruvengadam M. Harnessing Nature: Computational and Experimental Insights Into *Ipomoea obscura* Metabolites for Bladder Cancer Therapy. Chemistry and Biodiversity. 2025; 0: e00909.
[15] Dugganaboyana GK, Kannankumar MKG, Shivaramakrishna S, Raju MV, Chandrasekaran MK, Ahalliya

RM, Panneerselvam N, Palanisamy CP, Kanniappan GV. Phytochemical insights, antioxidant activity and therapeutic potential of Cassia senna against prostate cancer in Wistar albino rats. Discover Applied Sciences. 2025; 7:1206.
[16] Natarajan SR, Krishnamoorthy R, Alshuniaber MA, Gatasheh MK, Rajagopal P, Veeraraghavan VP, Palanisamy CP, Jayaraman S. KDM1A Facilitates Oncogenic Potential in Colorectal Cancer Progression Through the Activation of AXIN/GSK3β/β-Catenin Signaling Pathways: Evidence From Integrated Transcriptomics and In Vitro Studies. The Journal of Gene Medicine. 2025; 27(11): e70053.
[17] Guan T, Gong J, Lin J, Palanisamy CP, Jinjin Pei J, El-Aty AMA. Machine learning-driven multimodal optimization of selenium biotransformation and flavor profiling in fermented apple–Yacon functional beverages. Innovative Food Science & Emerging Technologies. 2025; 105: 104198.
[18] Natarajan SR, Krishnamoorthy R, Alshuniaber MA, Alsulami TS, Gatasheh MK, Rajagopal P, Palanisamy CP, Govindan R, Veeraraghavan VP, Jayaraman S. ABCE1 facilitates tumour progression via aerobic glycolysis and inhibits cell death in human colorectal cancer cells through the p53 signalling pathway. Scientific Reports. 2025; 15: 24674.
[19] Huang Y, Guo H, Liu Y, Jin W, Palanisamy CP, Pei J, Oz F, El-Aty AMA. Effects of Natural Polysaccharides on the Gut Microbiota Related to Human Metabolic Health. Molecular Nutrition & Food Research. 2025; 69:e202400792.
[20] Poornima K, Meenakshi K.C, Manikandan V.R, Shankari G, Prabhu D, Rathi M.A, Palanisamy CP, Balaji R, Gopalakrishnan V.K. Exploring the anticancer potential of Jerantinine A from *Tabernaemontana coronaria* against prostate, breast, and ovarian cancers: A computational approach. *Journal of Complementary and Integrative Medicine*, 2025 22(2): 363–372.
[21] Palanisamy CP, Poompradub S, Sansanaphongpricha K, Jayaraman S, Subramani K. Faridah Sonsudin gGreen synthesis of Nigella sativa-mediated silver nanoparticles for enhanced antibacterial activity and wound healing: Mechanistic insights and biomedical applications. Environmental Nanotechnology, Monitoring & Management. 2025; 24: 101085.
[22] Surendran N, Raju MV, Chandrasekaran MK, Ahalliya RM, Palanisamy CP, Chandrasekaran G, Kanniappan GV. Physicochemical characterization of starch from Maranta arundinacea L.(arrowroot) rhizomes and its inhibition of COX-2: In vivo validation. Bioactive Carbohydrates and Dietary Fibre. 2025; 33: 100465.
[23] Kannappan P, Chandrasekaran MK, Raju MV, Gopalakrishnan S, Dhamodharan P, Ahalliya RM, Palanisamy CP, Raju B, Kanniappan GV. Exploring the anticancer potential of Jerantinine A from Tabernaemontana coronaria against prostate, breast, and ovarian cancers: a computational approach. Journal of Complementary and Integrative Medicine. 2025; 22(02): 363-372.
[24] Pei J, Kumarasamy RV, Jayaraman S, Kanniappan GV, Long Q, Palanisamy CP. Quercetin-functionalized nanomaterials: Innovative therapeutic avenues for Alzheimer's disease management. Ageing Research Reviews. 2025; 104: 102665.
[25] Jayaraman S, Prasad M, Natarajan SR, Krishnamoorthy R, Alshuniaber MA, Gatasheh MK, Veeraraghavan VP, Rajagopal P, Palanisamy CP. Molecular mechanisms underlying the effects of beta-sitosterol on TGF-β1/Nrf2/SIRT1/p53-mediated signaling in the kidney of a high-fat diet and sucrose-induced type-2 diabetic rat. Chemico-Biological Interactions. 2025; 411: 111443.
[26] Huang Y, Guo H, Liu Y, Jin W, Palanisamy CP, Pei J, Oz F, El-Aty AMA. Effects of Natural Polysaccharides on the Gut Microbiota Related to Human Metabolic Health. Molecular Nutrition & Food Research. 2025; e202400792.
[27] Prabhakaran P, Palanisamy CP, Shanmugam A, Damodharan P, Swaminathan H, Devaraj D, Ahalliya RM, Kanniappan GV. Isolation, structural characterization, and molecular docking studies on the bioactive compound from n-Hexane extract of Emilia sonchifolia (L.) DC against the pancreatic cancer target Aurora 2 Kinase. Journal of Complementary and Integrative Medicine. 2024; 22(1): 0290.
[28] Jiang H, Kumarasamy RV, Pei J, Raju K, Kanniappan GV, Palanisamy CP. Integrating engineered nanomaterials with extracellular vesicles: Advancing targeted drug delivery and biomedical applications. Frontiers in Nanotechnology. 2024; 6: 1513683.
[29] Guo H, Liu Y, Wan T, Song D, Palanisamy CP, Geng J, Pei J, Özmen S, El-Aty AMA. Toward personalized cancer management: Role of precision nutrition–diet interventions. Journal of Functional Foods. 2024; 123: 106584.
[30] Natarajan SR, Krishnamoorthy R, Alshuniaber MA, Al-Anazi KM, Farah MA, Rajagopal P, Palanisamy CP, Veeraraghavan VP, Jayaraman S. Identification of FOXM1 as a novel protein biomarker and therapeutic target for colorectal cancer progression: Evidence from immune infiltration and bioinformatic analyses. International Journal of Biological Macromolecules. 282 (Part 4): 137201.
[31] Rajendran MS, Jayaraman S, Khan JM, Jasmine S, Prabhakaran RK, Raju MV, Chandrasekaran MK, Ahalliya RM, Kannappan P, Palanisamy CP, Kanniappan GV. Investigating the colon toxicity and carcinogenic role of monosodium glutamate compared with Dimethylhydrazine in male Wistar rats: Exploring the link to childhood colon cancer risk. Journal of King Saud University - Science. 2024; 36(11): 103507.
[32] Kumarasamy RV, Natarajan P, Umapathy VR, Roy JR, Rab SO, Saeed M, Panagal M, Mironescu M, Srinivasan GP, Palanisamy CP. Clinical Applications and Therapeutic Potentials of Advanced Nanoparticles: A Comprehensive Review on Completed Human Clinical Trials. Frontiers in Nanotechnology. 2024; 6:1479993.

[33] Jin W, Pei JJ, Roy JR, Jayaraman S, Ahalliya RM, Kanniappan GV, Mironescu M, Palanisamy CP. Comprehensive review on single-cell RNA sequencing: A new frontier in Alzheimer's disease research. Ageing Research Reviews. 2024; 274: 102454.
[34] Pei J, Palanisamy CP, Jayaraman S, Natarajan PM, Umapathy VR, Roy JR, Panagal M, Jayaraman S. Curcumin-loaded polymeric nanomaterials as a novel therapeutic strategy for Alzheimer's disease: A comprehensive review. Ageing Research Reviews. 2024; 99: 102393.
[35] Pei J, Palanisamy CP, Jayaraman S, Natarajan PM, Umapathy VR, Roy JR, Thalamati D, Ahalliya RM, Kanniappan GV, Mironescu M. A comprehensive review on starch-based Sustainable Edible Films Loaded with Bioactive Components for Food Packaging. International Journal of Biological macromolecules. 2024; 274 (Part-1): 133332.
[36] Palanisamy CP, poompradub S, Sansanaphongpricha K, Subramani K, Sonsudin F. Increased expression levels of PDGF and VEGF magnify the wound healing potential facilitated by biogenic synthesis of silver nanoparticles. Nano-Structures & Nano-Objects. 2024; 39: 101236.
[37] Pei J, Palanisamy CP, Jayaraman S, Natarajan PM, Umapathy VR, Roy JR, Thalamati D, Ahalliya RM, Kanniappan GV, Mironescu M. Proteomics Profiling of Extracellular Vesicle for Identification of Potential Biomarkers in Alzheimer's Disease: A Comprehensive Review. Ageing Research Reviews. 2024; 99: 102359.
[38] Xi J, Wang T, Xian P, Liu X, Du M, Yang H, Palanisamy CP, Lin W, Long Q. Proteomic insights uncover enhanced neurotherapeutic potential in conditioned mesenchymal stem cell-derived extracellular vesicles. Extracellular Vesicle. 2024; 3: 100037.
[39] Pei J, Natarajan PM, Umapathy VR, Swamikannu B, Sivaraman NM, Krishnasamy L, Palanisamy CP. Advancements in the synthesis and functionalization of zinc oxide-based nanomaterials for enhanced oral cancer therapy. Molecules. 2024; 29(11): 2706.
[40] Gatasheh MK, Natarajan SR, Krishnamoorthy R, Alsulami TS, Rajagopal P, Palanisamy CP, Veeraraghavan VP, Jayaraman S. Molecular analysis to identify novel potential biomarkers as drug targets in colorectal cancer therapy: an integrated bioinformatics analysis. Molecular and Cellular Oncology. 2024; 11(1): 2326699.
[41] Pei J, Yan Y, Jayaraman S, Rajagopal P, Natarajan PM, Umapathy VR, Gopathy S, Roy JR, Sadagopan CS, Thalamati D, Palanisamy CP, Mironescu M. A review on advancements in the application of starch-based nanomaterials in biomedicine: Precision drug delivery and cancer therapy. International Journal of Biological Macromolecules. 2024; 130746.
[42] Natarajan PM, Umapathy VR, Murali A, Swamikannu B. (2022). Computational Simulations of Identified marine-derived Natural Bioactive Compounds As Potential Inhibitors of Oral Cancer. Future Science OA. 2022; 8(3).
[43] Natarajan PM, Umapathy VR. Role of transcriptomics in the study of oral cancer. Frontiers in Oral Health. 2025; 6:1524364.
[44] Vidhyarekha U, Natarajan PM, Bhuminathan S, Sabarinathan J, Suba R, Vijayalakshmi P. Role of artificial intelligence in Oral Cancer. Advances in Public Health. 2024. 2024: 3664408.
[45] Ganesan A, Kumar NG, Natarajan PM, Gauthaman J. Automated classification of elongated styloid processes using deep learning models-an artificial intelligence diagnostics. Frontiers in Oral Health. 2025; 5: 1424840.
[46] Umapathy VR, Natarajan PM, Swamikannu B. Regenerative Strategies in Dentistry: Harnessing Stem Cells, Biomaterials and Bioactive Materials for Tissue Repair. Biomolecules. 2025; 15: 546.
[47] Natarajan PM. Dental Bioinformnatics-Current Scope and Future perspectives. Research Journal of Pharmacy and Technology. 2022;15(5):2351-6.
[48] Ganesan A, Kumar NG, Natarajan PM. Solanum trilobatum leaf extract-derived silver nanoparticles downregulate the PI3K/AKT/mTOR signaling pathway and attenuate oral squamous cell carcinoma cell proliferation. Journal of Herbmed Pharmacology. 2024; 13(2): 300-307.
[49] Perumal MKK, Renuka RR, Subbiah SK, Natarajan PM. Artificial intelligence-driven clinical decision support systems for early detection and precision therapy in oral cancer: a mini review. Frontiers in Oral Health. 2025; 6: 1592428.
[50] Ramesh E, Ganesan A, Lakshmi KC, Natarajan PM. Artificial intelligence-based diagnosis of oral leukoplakia using deep convolutional neural networks Xception and MobileNet-v2. Frontiers in Oral Health. 2025; 6: 1414524.
[51] Ganesan A, Kumar NG, Natarajan PM. Anticancer activity of silver nanoparticles synthesized from aqueous leaf extract of Solanum trilobatum (Purple fruit pea eggplant) on human oral cancer cells. Journal of Herbmed Pharmacololgy. 2024; 13(2): 260-268.
[52] Pei JJ, Perumal NC, Meng P, Long Q, Palanisamy CP. AI-assisted FTIR spectroscopic profiling of exosomes: Emerging frontiers in early detection of Alzheimer’s disease. Ageing Research Reviews. 2026; 103311.
[53] Raja FSD, Abraham L, Rangasamy K, Saikia K, Rathankumar AK, Mironescu M, Mironescu I, Palanisamy CP, Kanniappan GV. Next-Generation Microbiome Therapeutics: Psychobiotics and Fecal Microbiota Transplants (FMT) for Mental Health Treatment. Frontiers in Cellular and Infection Microbiology. 2026; 16: 1719357.
[54] Subramani K, Srinivasan S, Shanmugam P, Palanisamy CP, Sonsudin F, Poompradub S. Sustainable phytochemical mediated-ZnO nanoparticles derived from Crescentia cujete for toxicological evaluation and multifunctional environmental applications. Environmental Nanotechnology, Monitoring & Management. 2026; 26: 101180.

[55] Kunamalla RP, Panagal M, Palanisamy CP. Green-engineered multiscale starch/PVA nanofibrous scaffolds embedded with CuO nanoparticles from Sargassum ilicifolium for potent antimicrobial performance. Genetics and Molecular Research. 2026; 25(13s): 1-9.
[56] Dharmaprakash S, Gunasekaran VP, Sivaramakrishnan R, Kanniappan GV, Jayaraman S, Mironescu M, Rajabathar JR, Mironescu ID, Palanisamy CP. Marine macroalgae-mediated ultrasonic-assisted green synthesis of CuO nanoparticles embedded in starch/PVA electrospun nanoscaffolds for in vitro α-amylase and α-glucosidase inhibitory activity. Scientific Reports. 2026; 16: 26243.
[57] Surendran N, Chandrasekaran G, Raju MV, Chandrasekaran MK, Ahalliya RM, Palanisamy CP, Kanniappan GV, Arcot R, Alharbi NS, Thiruvengadam M. Anti-inflammatory potential of ethanolic extract of Maranta arundinacea L.: Insights from COX-2 modulation and oxidative stress analysis. South African Journal of Botany. 2026; 195: 142-151.
[58] Pei J, Senthilkumar MV, Hessini K, Subramaniyam S, Sivaramakrishnan R, Kanniappan GV, Jayaraman S, Palanisamy CP. Green fabrication of starch/PVA/CuO nanoscaffolds using marine macroalgae extract for enhanced anti-inflammatory activity. Sustainable Chemistry and Pharmacy. 2026; 51: 102397.
[59] Natarajan PM, Swamikannu B, Sivaraman NM, Stylin AGSQ. Prevention of Oral Cancer: A Comprehensive Guide. Journal of Pharmacy and Bioallied Sciences. 2024; 16(5): S4239-S4241.
[60] Umapathy V, Dhanavel A, Kesavan R, Natarajan PM, Bhuminathan S, Vijayalakshmi P. Anticancer Potential of the Principal Constituent of Piper nigrum, Piperine: A Comprehensive Review. Cureus. 2024; 16(2): e54425.
[61] Umapathy VR, Swamikannu B, Natarajan PM, Devi R, Nandini MS, Vimalarani, Vijayalakshmi P. In Silico Molecular Docking of Ocimum sanctum Phytochemicals: Targeting Key Biomarkers in Oral Cancer. Journal of Pharmacy and Bioallied Sciences. 2024; 16(5): S4792-S4799.
[62] Natarajan PM, Bhuminathan S, Rajan R, Bindu K, Loganathan K, Veerakumar R. The Crucial Role of Smoking Cessation in Preventing Oral Cancer. Journal of Pharmacy and Bioallied Sciences. 2024; 16(5): S4245-S4247.
[63] Swamikannu B, Umapathy VR, Natarajan PM, Nandini MS, Stylin AGSQ, Vimalarani V, Rajinikanth S. Unlocking the Therapeutic Benefits of Artemisia Annua: A Comprehensive Overview of its Medicinal Properties. Journal of Pharmacy and Bioallied Sciences. 2024; 16(5): S4248-S4253.
[64] Natarajan PM. Computational Studies on Recent Congeners of Fluoroquinolones and Nitroimidazoles for Their Use in Periodontal Therapy. Journal of Pharmacy and Bioallied Sciences. 2024; 16(5): S4731-S4740.
[65] Yadalam PK, Arumuganainar D, Natarajan PM, Ardila CM. Artificial intelligence-powered prediction of AIM-2 inflammasome sequences using transformers and graph attention networks in periodontal inflammation. Scientific Reports. 2025; 15: 8733.
[66] Yadalam PK, Chatterjee S, Natarajan PM, Ardila CM. Comparison of light gradient boosting and logistic r egression for interactomic hub genes in Porphyromonas gingivalis and Fusobacterium nucleatum-induced perio dontitis with Alzheimer's disease. Frontiers in Oral Health. 2025; 6:1463458.
[67] Natarajan PM, Bhuminathan S, Leela B, Bindu K, Loganathan K, Ramachandran V. Smoking and its Role in Oral Cancer. Journal of Pharmacy and Bioallied Sciences 16(5): S4242-S4244.
[68] Yadalam PK, Natarajan PM, Ardila CM. Variational graph autoencoder for reconstructed transcriptomic data associated with NLRP3 mediated pyroptosis in periodontitis. Scientific Reports. 2025; 15: 1962.
[69] Pei JJ, Yan Y, Palanisamy CP, Jayaraman S, Natarajan PM, Umapathy VR, Gopathy S, Roy JR, Sadagopan JC, Thalamati D, Mironescu M. Materials-based drug delivery approaches: Recent advances and future perspectives. Green Processing and Synthesis. 2024; 13: 20230094.
[70] Pei JJ, Deng W, Liu Y, Guo Y, Chen J, Abdu H, Khan MR, Palanisamy CP, El-Aty AM. A Comprehensive Review of Cornus officinalis: Health Benefits, Phytochemistry, and Pharmacological Effects for Functional Drug and Food Development. Frontiers in Nutrition. 2023; 10: 1309963.
[71] Alugoju P, Palanisamy CP, Anthikapalli NVA, Jayaraman S, Prasanskulab A, Chuchawankul S, Dyavaiah M, Tencomnao T. Exploring the anti-aging potential of natural products and plant extracts in budding yeast Saccharomyces cerevisiae: A review. F1000Research. 2023; 12: 1265.
[72] Lavanya M, Krishnamoorthy R, Alshuniaber MA, Manoharadas S, Palanisamy CP, Veeraraghavan VP, Jayaraman S, Rajagopal P, Padmini R. Formulation, characterization and evaluation of gelatin-syringic acid/zinc oxide nanocomposite for its effective anticancer, antioxidant and anti-inflammatory activities. Journal of King Saud University-Science. 2023; 35: 102909.
[73] Palanisamy CP, Poompradub S, Sansanaphongpricha K, Jayaraman S, Subramani K, Sonsudin F. Biosynthesis of silver nanoparticles (AgNPs) using ethanolic extract of Nigella sativa (L.) seeds promotes wound healing via PDGF and VEGF signalling pathways activation. Biocatalysis and Agricultural Biotechnology. 2023; 54: 102970.
[74] Prasad M, Jayaraman S, Natarajan SR, Veeraraghavan VP, Krishnamoorthy R, Gatasheh MK, Palanisamy CP, Elrobh M. Piperine modulates IR/Akt/GLUT4 pathways to mitigate insulin resistance: Evidence from animal and computational studies. International Journal of Biological Macromolecules. 2023; 253: 127242.
[75] Palanisamy CP, Pei JJ, Phaniendra A, Venkata AAN, Jayaraman S, Veeraragahavan VP, Sridevi G, Roy JR, Janaki CS, Thalamati D, Mironescu M, Luo Q, Chai Y, Long Q. New Strategy of Neurodegenerative Disease Treatment with Extracellular Vesicles (EVs) Derived from Mesenchymal Stem Cells (MSCs). *Theranostics*. 2023; 13(12):4138-4165. doi:10.7150/thno.83066.

[76] Palanisamy CP, Phaniendra A, Jayaraman S, Poompradub S. *Nigella sativa* L. seed extracts promotes wound healing progress by activating VEGF and PDGF signalling pathways: *An in vitro* and *in silico* study. *F1000 Research*. 2023; 12: 436.
[77] Pei JJ, Palanisamy CP, Phaniendra A, Venkata AAN, Natarajan PM, Umapathy VR, Swamikannu B, Jayaraman S, Rajagopal P, Poompradub S. A comprehensive review on bio-based materials for chronic diabetic wounds. *Molecules*. 2022; 28(2), 604.
[78] Palanisamy CP, Cui B, Zhang H, Gunasekaran VP, Ariyo A, Jayaraman S, Veeraraghavan V, Rajagopal P. A critical review on starch-based electrospun nanofibrous scaffolds for wound healing application. International Journal of Biological Macromolecules. 2022; 222 (Part: B): 1852-1860.